Neuron, Vol. 33, 23–34, January 3, 2002, Copyright ©2002 by Cell Press

Hoxb8 Is Required for Normal Grooming Behavior in Mice

Joy M. Greer and Mario R. Capecchi[1]
Howard Hughes Medical Institute
Department of Human Genetics
University of Utah School of Medicine
Salt Lake City, Utah 84112

Summary

Repertoires of grooming behaviors critical to survival are exhibited by most animal species, including humans. Genes that influence this complex behavior are unknown. We report that mice with disruptions of *Hoxb8* show, with 100% penetrance, excessive grooming leading to hair removal and lesions. Additionally, these mice excessively groom normal cagemates. We have been unable to detect any skin or PNS abnormalities in *Hoxb8* mutants. These observations suggest that the excessive, pathological grooming exhibited by these mice results from CNS abnormalities. Consistent with this interpretation, we demonstrate *Hoxb8* expression in regions of the adult mouse CNS previously implicated in the control of grooming. The aberrant behavior observed in *Hoxb8* mutants is not unlike that of humans suffering from the OC-spectrum disorder, trichotillomania. Interestingly, *Hoxb8* is expressed in regions of the CNS known as the "OCD-circuit."

Introduction

Grooming is an innate behavior that is represented across most animal species, including humans (Sachs, 1988). Care of one's own body surface, autogrooming, is a spontaneous behavior that generally occurs as a transition behavior between periods of rest and activity (Fentress, 1988). During grooming bouts in rodents, and many other mammalian species, a general pattern of cephalocaudal progression is observed, i.e., the head is groomed first, followed by the body region, and finally the anogenital region and tail. The most highly predictable stereotyped action sequence is described as an "idealized syntactic grooming chain" (Berridge et al., 1987). Analysis of grooming behaviors in rodents suggests that pattern-generating signals originating within the CNS organize the physical movements performed during individual grooming bouts (Berridge et al., 1987; Berridge and Whishaw, 1992; Richmond, 1980). Multiple regions of the brain, but most notably the brainstem and striatum, appear to be involved in implementing the syntactic grooming chain (Aldridge et al., 1993; Berntson et al., 1988; Berridge, 1989a; Berridge and Whishaw, 1992).

Obsessive-compulsive disorder (OCD) in humans is a condition that is often characterized by excessive behaviors dealing with cleanliness, including grooming. Epidemiological studies using cross-national representations have indicated that this disorder is quite common in humans, with a prevalence rate ranging from 1.9–2.5 per 100 in seven separate international communities (Horwath and Weissman, 2000). However, genes that influence this complex behavior have yet to be identified. In this context, it is of particular interest that mice homozygous for a loss-of-function mutation in *Hoxb8* show excessive pathological grooming behavior, leading to hair removal and self-inflicted wounds at over-groomed sites.

Hoxb8 is a member of the mammalian *Hox* (Homeobox-containing) complex, a group of 39 transcription factors best known for their roles during early development in providing positional information along the anteroposterior axis (Capecchi, 1997). Like most murine *Hox* genes, *Hoxb8* is first expressed in the embryonic primitive streak at E7.5. During the next 24 hr, *Hoxb8* expression progresses anteriorly so that by E8.5 it is expressed to the level of somite 5 in the neural ectoderm, and to the somite 10/11 boundary in mesoderm (Deschamps and Wijgerde, 1993). By embryonic day 11.5 (E11.5), *Hoxb8* is expressed in the developing spinal ganglia and throughout the spinal cord to the level of the hindbrain/spinal cord boundary (Deschamps and Wijgerde, 1993). The functions of *Hox* genes, however, are not restricted to embryonic development. For example, *Hoxc13* is required for all hair formation in adult mice, and *Hox9* genes are needed for maturation of breast tissue in pregnant females (Chen and Capecchi, 1999; Godwin and Capecchi, 1998). Additionally, we have also found that numerous *Hox* genes are expressed in the adult CNS (unpublished results; see also Le Mouellic et al., 1992; Odenwald et al., 1987). Herein we demonstrate that *Hoxb8* is extensively expressed in the adult CNS in regions previously implicated in the control of rodent grooming behavior (Aldridge et al., 1993; Berntson et al., 1988; Berridge, 1989a; Berridge and Fentress, 1987b; Berridge and Whishaw, 1992; Cannon, 1992; Cromwell and Berridge, 1996; McGrath et al., 1999; Robertson et al., 1999).

In this report, we describe two *Hoxb8* loss-of-function alleles. Both contain a nonsense mutation in the first exon; one also contains a floxed *neo*^{r} cassette in the second exon (see Figure 1), and the other contains a *loxP* site in exon 2. *Hoxb8* homozygous mutant mice show with 100% penetrance and in two distinct genetic backgrounds an excessive grooming behavior that is characterized by extensive hair removal and deep skin wounds. Characterization of the grooming behavior in the home cage, as well as during induced grooming assays, showed that *Hoxb8* mutant mice spend almost twice the time grooming as wild-type siblings. In addition, these mutant mice excessively groom control cagemates.

Results

Generation of *Hoxb8*^{neo} and *Hoxb8*^{lox} Mutant Mice

A replacement type gene targeting vector containing mutations in both exons of *Hoxb8* was constructed

[1] Correspondence: mario.capecchi@genetics.utah.edu

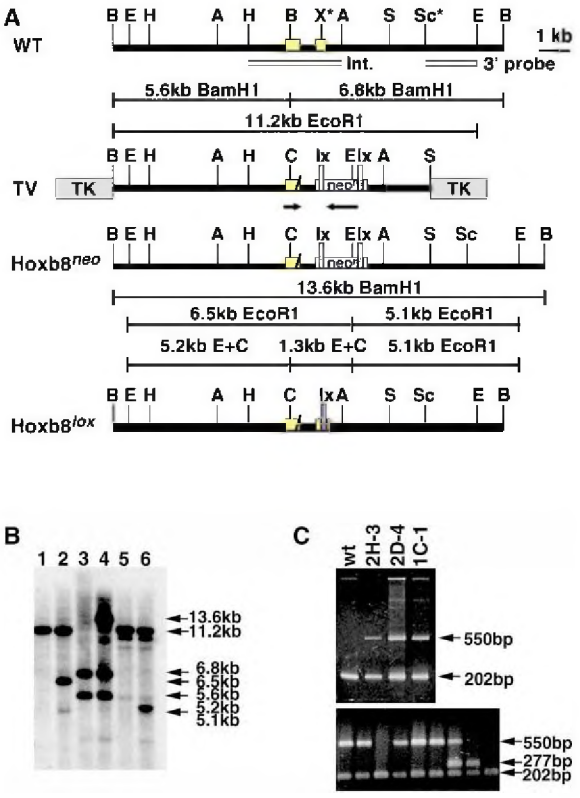

Figure 1. Disruption of *Hoxb8* and Genotypic Analysis of ES Cell Lines and *Hoxb8* Mutant Animals

(A) Representations of the *Hoxb8* genomic locus (WT), the targeting vector (TV), the *Hoxb8*^{neo} allele, and the *Hoxb8*^{lox} allele are shown. The two exons of *Hoxb8* are represented as yellow boxes, the *neo*^{r} gene by the blue box, and the *lox* sites are shown in purple. The arrows indicate the direction of transcription for *Hoxb8* and the *neo*^{r} gene. The diagonal line in the first exon represents the introduced translational stop site. The location of the two probes used to screen ES cell lines are shown in gray. The restriction digests and subsequent fragment lengths used to identify homologous recombinants are shown below the wild-type and *Hoxb8*^{neo} alleles.

(B) shows a Southern blot analysis of DNA from wild-type (lanes 1, 3, and 5) and the homologous recombinant ES cell line 1c-1 (lanes 2, 4, and 6). The DNAs were digested with EcoR1 (lanes 1 and 2), BamH1 (lanes 3 and 4), and EcoR1 + Cla1 (lanes 5 and 6). The blot was probed with an internal probe, a 3.0 kb HindIII-Asp718 fragment. Hybridization with this probe detects the endogenous 11.2 kb EcoR1 fragment, or the 6.5 kb and 5.1 kb mutant EcoR1 fragments, respectively (lanes 1 and 2). Destruction of the unique BamH1 site in the first exon results in a single 13.6 kb fragment (lane 4) rather than the endogenous 5.6 kb and the 6.8 kb fragments (lane 3). The presence of the introduced Cla1 site is demonstrated by double digestion with EcoR1 and Cla1. Since there are no endogenous Cla1 sites, only the EcoR1 fragment is detected in wild-type ES cell DNA (lane 5); however, three fragments are detected in the mutant cell line following hybridization with the internal probe: a 5.2 kb Eco + Cla fragment, a 1.3 kb Eco + Cla fragment (not shown), and the 5.1 kb EcoR1 fragment (lane 6).

(C) PCR analysis of the three mutant ES cell lines (upper panel) and genotype analysis of tail DNA from progeny subjected to Cre microinjection (lower panel) is shown. Amplification (see Experimental Procedures) of the wild-type allele results in a band at 202 bp, the *Hoxb8*^{neo} allele at 550 bp, and the *Hoxb8*^{lox} allele at 277 bp. Note the chimeric animal that contains all three alleles. A, Asp718; B, BamH1; C, Cla1; E, EcoR1; H, HindIII; Ix, *lox*; S, Sal1; Sc, Sac1; X, Xmn1. * indicates that multiple sites exist and are not all represented.

(Thomas and Capecchi, 1987). The first mutation is a frameshift mutation resulting in a premature translation stop codon within the first exon (Figure 1A). The second mutation was an insertion of a floxed *pMC1neo*^{r} cassette into the homeodomain encoded by the second exon. The targeting vector was electroporated into embryo-derived stem (ES) cells, followed by positive-negative selection to enrich for cells containing the *Hoxb8* mutant allele (Mansour et al., 1988). Southern transfer analysis was used to identify and characterize three ES cell lines containing the desired *Hoxb8* targeted mutations (Figure 1B). Two of these cell lines were used to generate chimeric males that passed the mutations onto their offspring, giving rise to the *Hoxb8*^{neo} colonies. All subsequent progeny were genotyped by PCR assays using tail DNA (Figure 1C). Removal of the *neo*^{r} cassette was accomplished by injection of *pMC1Cre* (Araki et al., 1995) into the male pronucleus of eggs fertilized by *Hoxb8*^{neo} male heterozygotes (Figure 1C) to generate the *Hoxb8*^{lox} colony. Mice homozygous for either mutant allele, *Hoxb8*^{neo} or *Hoxb8*^{lox}, should not produce any Hoxb8 protein since both alleles contain nonsense mutations in both exon 1 and exon 2 of this gene.

Allele-Specific Skeletal Phenotype

Loss-of-function alleles of individual *Hox* genes often result in patterning defects of the axial skeleton. To determine if *Hoxb8* is required for this process, we examined skeletal preparations of homozygous mutant newborn pups from both the *Hoxb8*^{neo} and *Hoxb8*^{lox} colonies. In wild-type mice, the first rib normally is formed as a ventrolateral projection that originates from the sclerotome adjacent to the first thoracic vertebra. This rib articulates with the top of an independently formed sternum (Figure 2A). Examination of 62 *Hoxb8*^{neo} homozygous mutants revealed defects in the formation of the first rib in 46 (74%) of the mutants. In 75% of these 46, the defect was bilateral. The expressivity of this defect ranged from a relatively mild form in which the first and second ribs were fused near their attachment point at the sternum, to a severe defect characterized by complete absence of a rib adjacent to the first thoracic vertebra (Figures 2B and 2D).

In contrast to the *Hoxb8*^{neo} mutant homozygous phenotype, no defects in the formation of the first rib were found in skeleton preparations of 35 *Hoxb8*^{lox} homozygous mutants (Figure 2C). The only difference between these two alleles is the presence of the *neo*^{r} cassette in the homeodomain of the *Hoxb8* locus, implicating the *neo*^{r} cassette as the cause of the skeletal anomalies.

Previous examination of *Hoxb9* homozygous mutants had revealed a defect in the formation of the first thoracic rib (Chen and Capecchi, 1997). Because the rib defects observed in *Hoxb8*^{neo} homozygotes resembled those described for *Hoxb9* homozygous mutant animals, the embryonic expression pattern of this gene in the *Hoxb8* mutants was examined. At E9.5, *Hoxb9* is expressed in wild-type embryos to the level of somite 7-8 (Figure 2E) (Chen and Capecchi, 1997). Sixty-six percent (6/9) of E9.5 *Hoxb8*^{neo} homozygous mutant embryos displayed an abnormal pattern of *Hoxb9* expression, with its expression being shifted posteriorly by one somite (Figure 2F). This alteration was never observed in E9.5 *Hoxb8*^{lox}

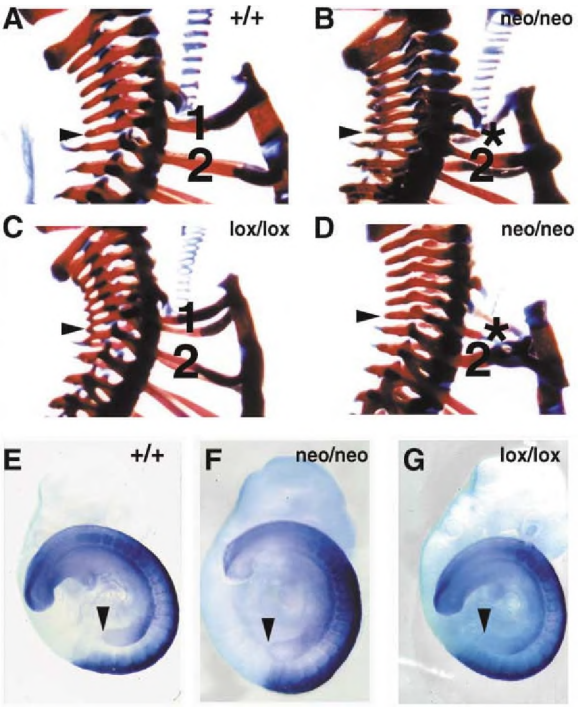

Figure 2. Skeletal Phenotype and Altered Gene Expression Induced by the *Neo*^{r} Gene

(A–D) Skeletal preparations of wild-type (A), *Hoxb8*$^{neo/neo}$ (B and D), and *Hoxb8*$^{lox/lox}$ (C) animals are shown. The black arrowhead marks the first thoracic vertebrae (T1) in each animal. The numbers 1 and 2 designate the 1st and 2nd ribs, respectively. Note the malformations in the first thoracic rib in the *Hoxb8*$^{neo/neo}$ animals denoted by the asterisk.

(E)–(G) show expression pattern of *Hoxb9* in wild-type (E), *Hoxb8*$^{neo/neo}$ (F), and *Hoxb8*$^{lox/lox}$ (G) embryos at E9.5. The black arrowhead marks the anterior edge of the forelimb bud in each panel.

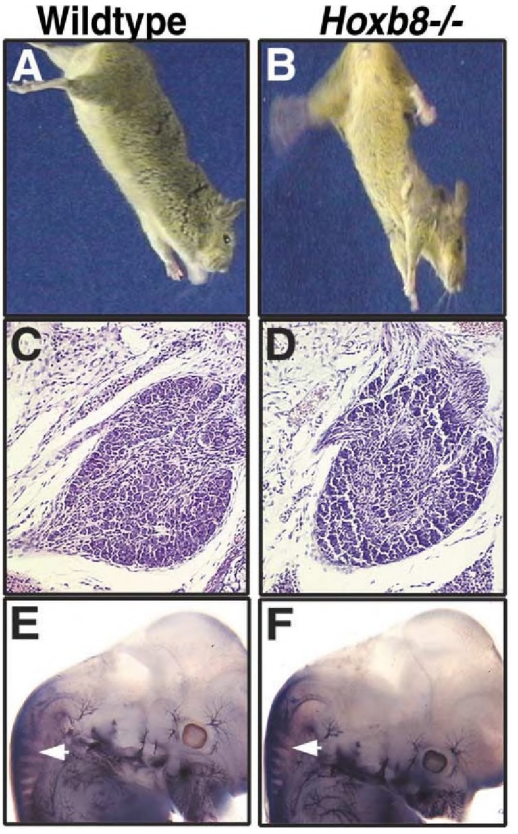

Figure 3. Normal Forearm Clasping Reflex and C2 Ganglia in *Hoxb8*$^{-/-}$ Mice

(A) and (B) demonstrate the normal reaching reflex in both wild-type (A) and *Hoxb8*$^{-/-}$ (B) animals when they are lifted by the tail from their cage. (C and D) show transverse sections demonstrating normal size and morphology of the C2 dorsal root ganglia in newborn wild-type (A) and *Hoxb8*$^{-/-}$ (B) animals. (E and F) Anti-neurofilament staining of E13.5 wild-type (E) and *Hoxb8*$^{-/-}$ (F) animals is shown. The arrow indicates the developing 2nd dorsal root ganglion.

homozygous embryos (6/6; Figure 2G). No changes in the *Hoxb9* expression pattern were observed in *Hoxb8*^{neo} homozygous mutant embryos examined at E10.5, E11.5, and E12.5 (data not shown).

Previous skeletal analysis of *Hoxb6* mutant homozygotes revealed that 50% of these animals showed similar first rib malformations. In situ hybridization of six E9.5 *Hoxb8*^{neo} embryos revealed a posterior shift of *Hoxb6* expression by one somite in 30% of these embryos (data not shown). No alteration of *Hoxb6* expression was observed in E9.5 *Hoxb8*^{lox} mutant homozygous embryos. In addition, *Hoxb6* expression was examined in E10.5 and E12.5 homozygous mutant embryos from both colonies and no additional changes in expression relative to wild-type controls were observed (data not shown).

From these data, we conclude that the presence of the bacterial *neo*^{r} gene in the *Hoxb8* locus interferes with the expression patterns of neighboring *Hox* genes, which in turn may be responsible for the first thoracic rib malformations in these mutant animals. Removal of the *neo*^{r} cassette from *Hoxb8*^{neo} animals eliminates the *Hoxb6* and *Hoxb9* misexpression, as well as the rib defects.

Deschamps and her colleagues have also reported on a loss-of-function allele of *Hoxb8* (van den Akker et al., 1999). The phenotype of their mutant animals includes axial skeleton abnormalities and a defective forearm clasping reflex. The latter defect was attributed to aplasia of the spinal dorsal root ganglion, C2. They also noted that one-third of their *Hoxb8*$^{-/-}$ mice had self-inflicted lesions, but did not comment on their cause. The skeletal abnormalities they reported were very similar to those described above for our *Hoxb8*^{neo} mutants. In that case, the abnormalities cannot be attributed to a *neo*^{r} affect since the *neo*^{r} cassette was removed from their mutant locus. However, their *Hoxb8* mutant allele retains the bacterial *lacZ* gene, which they used as a reporter for monitoring *Hoxb8* expression. The presence of the bacterial *lacZ* gene has been shown to interfere with the expression of neighboring genes, in a number of different contexts, in mice and cultured mammalian cells (Cohen-Tannoudji et al., 2000; Guy et al., 1997; Thorey et al., 1993). This may explain the similarities between the *Hoxb8*^{neo} and *Hoxb8*^{lacZ} alleles.

Our *Hoxb8*^{lox} mutant homozygotes also do not exhibit forelimb clasping defects nor hypoplasia of the C2 dorsal root ganglion (Figure 3). The latter defects in mice

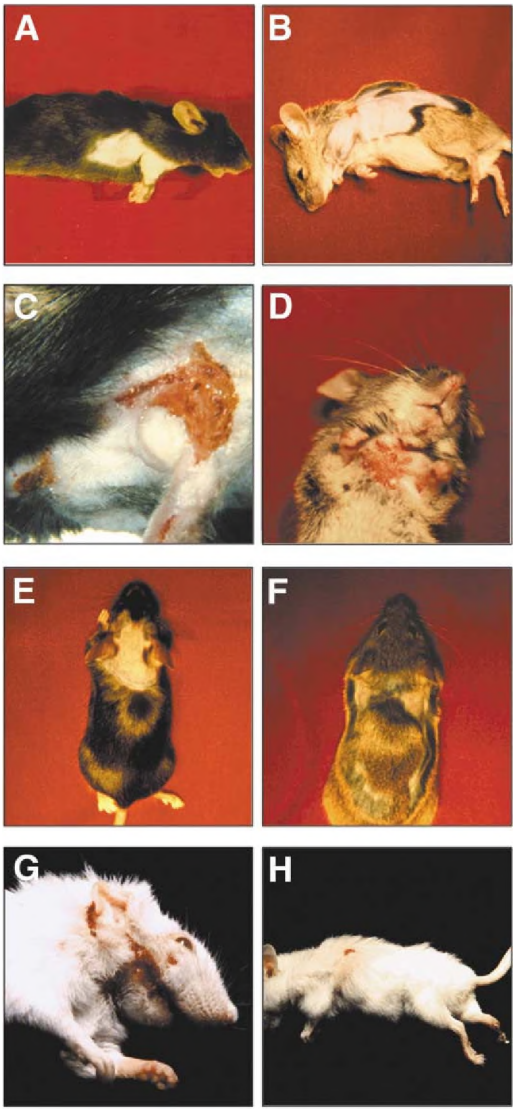

Figure 4. Mutilation Resulting From Excessive Grooming by *Hoxb8* Mutants

(A and B) Two *Hoxb8*$^{-/-}$ animals that have removed their body hair from lateral regions, without creating large lesions, are shown. (C) and (D) show examples of self-created lesions on the lateral and ventral body walls of two *Hoxb8*$^{-/-}$ animals. (E and F) Wild-type animals that were each housed with a different *Hoxb8*$^{-/-}$ sibling are shown. Note the hair loss resulting from excessive grooming by the *Hoxb8*$^{-/-}$ animal. (G) and (H) show self-created lesions resulting from excessive grooming in two different *Hoxb8*$^{-/-}$ animals from the Swiss genetic background. Note the mutilation of the hind paw in (H).

with the *Hoxb8*^{lacZ} mutant allele may also be attributable to misexpression of neighboring *Hox* genes induced by the presence of the bacterial *lacZ* gene. Since our *Hoxb8* mutant allele does not show defects either in the formation or maintenance of this dorsal root ganglia, it is unlikely that the behavioral abnormalities to be described below can be attributed to defects in these ganglia. Moreover, the anatomical regions affected by this behavior extend well beyond the dermatome map for the C2 dorsal root ganglion (see Figure 4).

Hair Removal Phenotype

All further discussions of phenotypic analysis will refer to the *Hoxb8*^{lox} strain only. During maintenance of these mice, it was observed that individually housed *Hoxb8* homozygous mutants displayed large bald patches on their lateral and ventral body surfaces. The extent of hair loss varied, from mice that displayed bald spots to the more severely affected animals that also had deep open wounds (Figures 4A–4D). Examination of mutant mice revealed significant amounts of body hair trapped between the gums and teeth, and present in their stomachs, suggesting that the mutant mice actively removed their own hair.

Analysis of Skin

Two potential physical explanations for this phenotype are an absence of afferent sensation or an inherent underlying irritation. To determine if those mice had normal cutaneous sensation, the animals were tested for their reactions to heat and cold, hard and soft pressure, as well as pain. All of the *Hoxb8* homozygous mutant mice displayed normal reactions to these stimuli (data not shown). In addition, immunostaining of E13.5 embryos with anti-neurofilament antibody and adult skin sections with a monoclonal antibody to the neuron-specific ubiquitin hydrolase, PGP9.5, failed to demonstrate any differences in the amount of peripheral nerve innervation in the mutant animals relative to control siblings (data not shown).

Histological analysis of skin taken from hairless body regions of *Hoxb8* mutant mice demonstrated a thickening of the epidermis when compared with similarly located skin of wild-type littermates (Figures 5A and 5B). This thickening, however, was only observed in older mice with hairless patches ($n = 20$). When skin from the ventral region of 2- and 3-week-old control and mutant littermates ($n = 18$ for each stage) was examined, no differences were observed (data not shown). These observations suggest that the thickening of the epidermis in affected mice is the result of the hair removal and wound healing, and not the cause of the behavior.

Physical examination of the skin did not reveal any inflammation of the area where hair had been removed except in regions containing lesions (Figure 5C). In addition, histological analysis of skin from mutant animals ($n = 20$) did not reveal evidence of lymphocyte and granulocyte infiltration or mast cell degranulation. Thus, an inflammatory reaction does not explain the hair removal phenotype (Figure 5D).

Home Cage Behavioral Analysis

To determine the conditions under which the *Hoxb8* mutant mice removed their body hair, individual mice from seven littermate pairs, each comprising one wild-type and one homozygous mutant, were videotaped for a single 24 hr period in their home cages. Twelve hours of videotape, in three four-hour blocks spread evenly throughout the day, were examined for each animal and scored for displays of innate behaviors including eating, drinking, sleeping, and grooming. Most of the behaviors were indistinguishable in wild-type and mutant mice. For example, the amounts of time spent eating (Figure 6A) and the frequency of eating were the same. Times

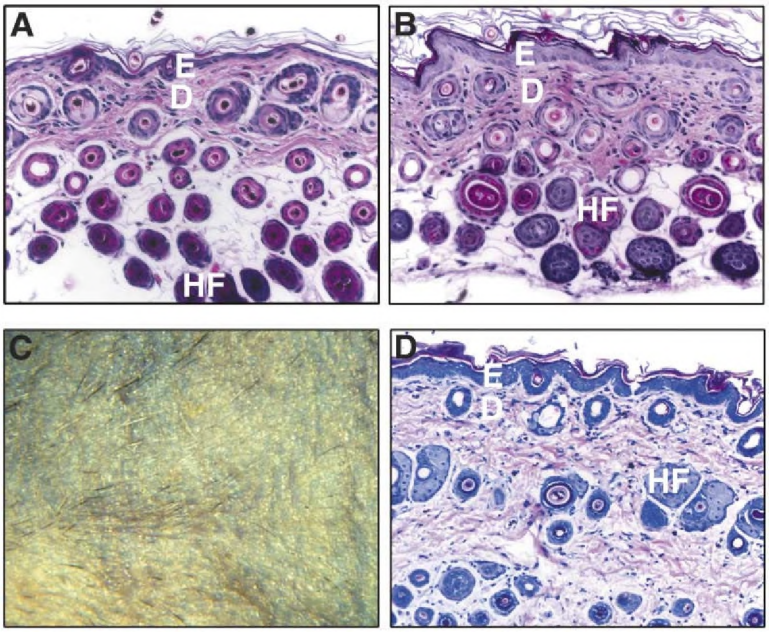

Figure 5. Examination of Affected Skin from *Hoxb8*$^{-/-}$ Animals

(A and B) H & E stained sections of skin prepared from the shoulder regions of wild-type (A) and *Hoxb8*$^{-/-}$ (B) adult animals are shown. The mutant animal had removed all the hair from this region prior to sample preparation. Note the thickening of the epidermis in the mutant animal. (C) shows a closeup photograph of skin from the chest region exposed by a mutant animal. (D) A Giemsa stained section of exposed skin from a *Hoxb8*$^{-/-}$ animal is shown. E, epidermis; D, dermis; HF, hair follicle.

spent drinking, climbing, hanging from the wire tops, or visitation to different regions of the cage were similar for the wild-type and mutant mice, all suggesting that the *Hoxb8* mutant homozygotes appear to have normal motor control. In addition, rearing and nest building appeared normal.

In contrast, when home cage grooming behaviors were analyzed, significant differences were found between the *Hoxb8* mutants and their control siblings (Figure 6B). When the fraction of grooming time was calculated, the *Hoxb8* mutant animals were found to spend almost twice as much time engaged in grooming behaviors as compared with their control siblings (P value 0.009 using the standard t test). In addition, the mutant animals initiated grooming sequences more frequently than did controls (Figure 6C). Although the mutant animals spent more time than controls engaged in grooming behaviors, it should be noted that the grooming sequences occurred within a normal context, i.e., as a transitional behavior between periods of rest and activity. Also, the mutant animals groomed all regions of their bodies and did not appear to have difficulties performing these actions. Although we have not yet quantified the total amount of time spent grooming during each phase of the syntactic chain, or other grooming sequences not involving the full syntactic chain pattern, it is readily apparent that the *Hoxb8* mutant homozygotes spend excessive time, relative to littermate controls, on body licking, or phase 4 of the syntactic chains. The excessive body licking and biting shown by these *Hoxb8* mutant mice accounts for their extensive hair loss and self-inflicted wounds.

Mutant animals spent on average 1 hr less time sleeping than did controls (Figure 6D). Since long periods of grooming generally precede periods of rest, the difference in the amount of time spent resting/sleeping may reflect a consequence of the excessive grooming.

Hoxb8 Excessive Grooming Includes a Social Component

A social component of the grooming behavior was also observed. When *Hoxb8* mutant mice were housed with control littermates, the control animals showed large bald patches on their backs and the tops of their heads (Figures 4E and 4F). Interestingly, the whiskers and facial regions of the control littermates were not excessively barbered, a behavior used by mice to establish dominance (Sarna et al., 2000; Strozik and Festing, 1981). Videotape analysis showed that these control animals were excessively groomed by the *Hoxb8* mutant animals.

Induced Grooming Analysis

Previous studies of rodent grooming behaviors have demonstrated that misting with water artificially stimulates these behaviors (Berridge et al., 1987). Ten control and mutant sib pairs were individually misted with water and videotaped for 20 min on 5 consecutive days. The *Hoxb8* mutants spent approximately twice as much time engaged in induced grooming behaviors as did their control littermates (Figure 6E).

Behavioral Analysis in a Second Genetic Background

To ensure that the single *Hox* gene mutation was responsible for the excessive grooming behavior, we backcrossed *Hoxb8* mutant mice from the F1 generation (C57BL6J/Sv129) to Swiss-Webster (SWR/J) mice for five generations. In this new genetic background, the excessive grooming behavior was also observed in all of the homozygous mutants using both the home cage and the induced grooming assays. Indeed, with the induced grooming assay, the homozygous mutants were once again found to spend approximately twice as much time grooming as did control siblings (Figure 6F). Visual

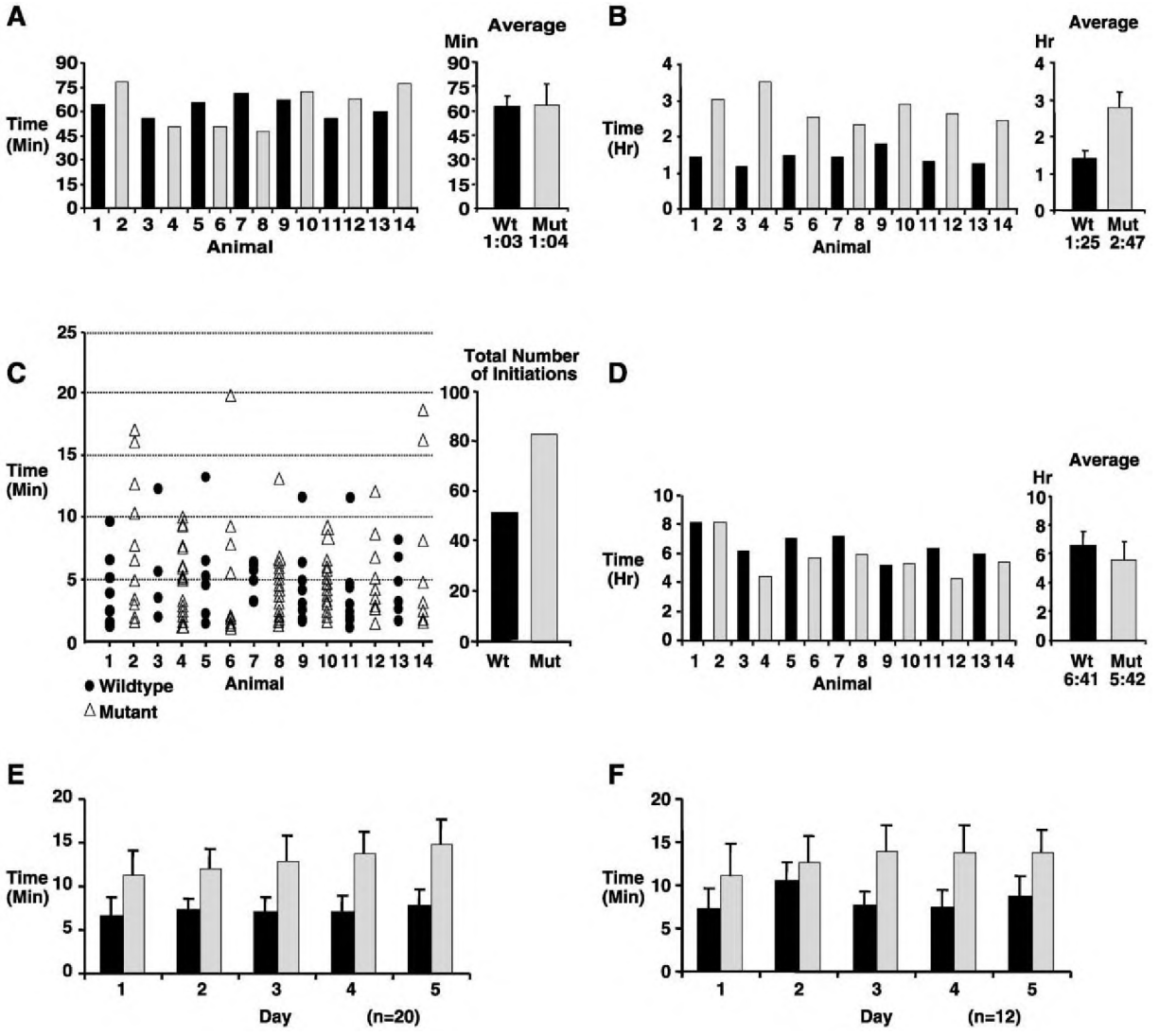

Figure 6. Behavior Analysis of *Hoxb8* Mutant Animals

(A, B, and D) Home cage analysis of the eating (A), grooming (B), and sleeping (D) patterns of the 14 animals observed is shown. The graph on the left side of each panel demonstrates the total amount of time each animal spent engaged in that activity during the 12 hr analysis period. Each set of two animals (i.e., 1 and 2, 3 and 4, etc.) represents a sex-matched wild-type and mutant sib pair. Animals 1–6 were females, whereas animals 7–14 were males. On the right side of each panel, the average amount of time the wild-type animals spent engaged in each activity is compared to the average amount of time the mutant animals spent engaged in the same activity. In all of the panels, the error bars denote standard deviation. Wild-type animals are denoted using black bars, mutant animals using gray. Note the near 2-fold discrepancy when the average amount of time spent grooming for wild-type and mutant animals is compared. Additionally, this pattern is consistent for each of the sib pairs tested, as demonstrated by the individual analyses on the left. (C) shows a representation of total number of grooming bouts observed for each animal during a single 4 hr time period. The animals used are the same as in (A), (B), and (D). On the left axis, time is represented in minutes. Each black dot (wild-type) or open triangle (mutant) represents a single grooming bout by that animal. The duration of each individual grooming bout corresponds to the number of minutes on the left axis. (E–F) Results of the induced grooming assay. (E) shows a comparison of the average amount of time ten wild-type and mutant sib pairs (20 animals total) spent grooming during the 20 min analysis period on each of five consecutive days. (F) Results of the induced grooming assay using six sib pairs from the SWR/J genetic background.

inspection of these animals showed that the *Hoxb8* homozygous mutant animals also removed their body hair and had self-inflicted skin lesions (Figures 4G and 4H) (for movies of mice grooming themselves, see Supplemental Data at http://www.neuron.org/cgi/content/full/33/1/23/DC1).

Expression Pattern of *Hoxb8* in the Adult CNS

To determine whether *Hoxb8* is expressed in the adult CNS, we assayed for the presence of *Hoxb8* mRNA by an RT-PCR assay. In 16-week-old wild-type animals, the expected 542 bp fragment was amplified from the cervical spinal cord, the brainstem, and the forebrain (Figure 7). When this RT-PCR assay was carried out with RNA isolated from the entire brain of adult *Hoxb8* homozygous mutant animals, a 617 bp fragment representing the *Hoxb8* mutant allele (542 bp plus a 34 bp *loxP* site surrounded by 37 bp of linker sequence and a 4 bp insertion in exon one) was amplified (Figure 7). Fragments of both sizes were amplified from brains of

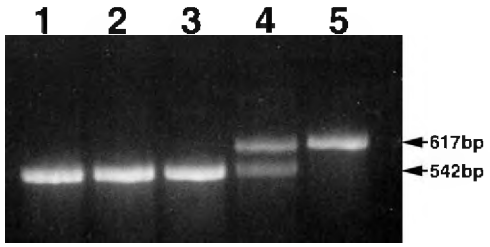

Figure 7. Amplification of *Hoxb8* Transcripts from the Adult CNS

RT-PCR amplification of *Hoxb8* transcripts using RNA isolated from the cervical spinal cord (lane 1), the brain stem (lane 2), and the entire brain following removal of the brain stem (lane 3) from wild-type adult animals. The size of the fragment amplified from the wild-type allele is 542 bp. Lane 4 demonstrates amplification of transcripts generated from both the wild-type and mutant alleles using RNA isolated from whole brains of *Hoxb8* heterozygous animals, while lane 5 demonstrates expression of only the mutant allele (617 bp) when RNA was isolated from the entire brain of *Hoxb8* homozygous mutant animals. Interestingly, although the *Hoxb8* mutant allele contains a nonsense codon in the first exon, the message is not degraded more rapidly than normal message. We believe that the reason the mutant message is not turned over more rapidly is that the nonsense codon is too close to the intron splice donor site to function as an effective signal for messenger RNA degradation.

heterozygous animals (Figure 7). Sequence analysis of the two PCR fragments confirmed that the 542 bp fragment was identical to that reported for *Hoxb8* (GenBank Accession number X13721), whereas the 617 bp fragment was found to contain both of the targeted mutations. These results demonstrate two important points: first, *Hoxb8* is expressed within the CNS of adult mice; second, the cells that would normally express *Hoxb8* are still present in the adult CNS of mutant animals. This does not imply that these cells are normal with respect to function. The mutant phenotype and the *Hoxb8* expression pattern suggest that this protein may participate in an integrative role during the modulation of motor and sensory information at multiple levels of the CNS. Although the mutant cells are still present, the data suggests that these cells may be defective in their integrative or interpretive capacity.

Cellular Localization of *Hoxb8* Transcripts in the Adult CNS

To determine the cellular distribution of *Hoxb8* expression within the adult CNS, we performed in situ hybridization using an antisense riboprobe from the 3′ untranslated region of *Hoxb8*. Sense strand hybridization to adjacent sections served as controls. *Hoxb8* expression was found in a number of regions within the wild-type adult CNS, including the olfactory bulb, the basal ganglia, the hippocampus, the cortex, the cerebellum, and the brain stem (Figure 8). In the olfactory bulb, *Hoxb8* expression is strongest in cells within the mitral cell layer (MiL) (Figures 8A–8C). A few *Hoxb8*-expressing cells are also seen within the external plexiform layer (EPL) and the granule cell layer (GrL). The caudate-putamen (neostriatum) region of the basal ganglia also contains *Hoxb8*-expressing cells (Figures 8D–8F).

Within the hippocampus, *Hoxb8* expression is restricted to the pyramidal cell layer in the CA1-CA3 region and the granule cell layer of the dentate gyrus (DG) (Figures 8G–8I). The cerebral cortex contains *Hoxb8*-expressing cells within layers 2–6. Although this expression pattern extends throughout the entire cortex, of particular interest is that the region with strongest expression includes the orbitofrontal (OFC) and anterior cingulate cortex (CCx) (Figures 8J–8L; 8M–8O). In the cerebellum, *Hoxb8* expression can be localized both to Purkinje cells and to basket cells (data not shown). In the brain stem, *Hoxb8* is expressed in cells throughout the reticular formation (RF) as well as in cells of the cranial ganglia (Figures 8P–8R). Examination of *Hoxb8* expression in adult brain sections from both hetero- and homozygous mutant animals showed identical expression patterns (data not shown). These expression patterns are consistent with studies that have linked grooming behavior in rodents to multiple regions of the brain, including the olfactory bulb, brain stem, hippocampus, frontal cortex, and caudate-putamen region of the basal ganglia (Aldridge et al., 1993; Berntson et al., 1988; Berridge, 1989a; Berridge and Fentress, 1987b; Berridge and Whishaw, 1992; Cannon, 1992; Cromwell and Berridge, 1996; McGrath et al., 1999; Robertson et al., 1999). It is also of special interest that *Hoxb8* is expressed in what has become known as the "OCD circuit," the orbitofrontal cortex, the anterior cingulate cortex, and the caudate nucleus because functional studies suggest that in OCD patients, there is abnormal metabolic activity within the cells of this circuit (for review, see Graybiel and Rauch, 2000).

Discussion

We have demonstrated that adult mice homozygous for a loss-of-function allele of *Hoxb8* display abnormal grooming behaviors. Not only does this represent a novel phenotype not previously associated with mutations in this gene, it demonstrates a novel role for a member of the *Hox* complex, a family of genes thought to be involved primarily in establishing the mammalian body plan.

Our study differs significantly from those published previously by van den Akker et al. (1999). They reported that the $Hoxb8^{lacZ}$ homozygous mutant mice have axial skeletal defects and an abnormal forearm clasping reflex that was attributed to the loss of the spinal dorsal root ganglion C2. However, van den Akker et al. did note that one-third of their $Hoxb8^{-/-}$ mice had self-inflicted skin lesions. In contrast, mice homozygous for our *Hoxb8* mutant allele, which has a nonsense mutation in the first exon and a *loxP* site in the second exon, showed no skeletal, forearm clasping, or dorsal root ganglia defects, but did show, with 100% penetrance and in two distinct genetic backgrounds, excessive grooming behavior and associated pathology. As argued in the Results, the marked differences in the skeletal and forelimb defects may reflect the presence of the bacterial *lacZ* gene in the Deschamps *Hoxb8* mutant allele (Cohen-Tannoudji et al., 2000; Guy et al., 1997; Thorey et al., 1993).

Numerous studies have demonstrated that, in rodents, grooming is an innate preprogrammed behavior (Sachs, 1988). This implies that the neuronal networks that regulate grooming behaviors are specified using a genetic program. Our behavioral analyses of *Hoxb8*

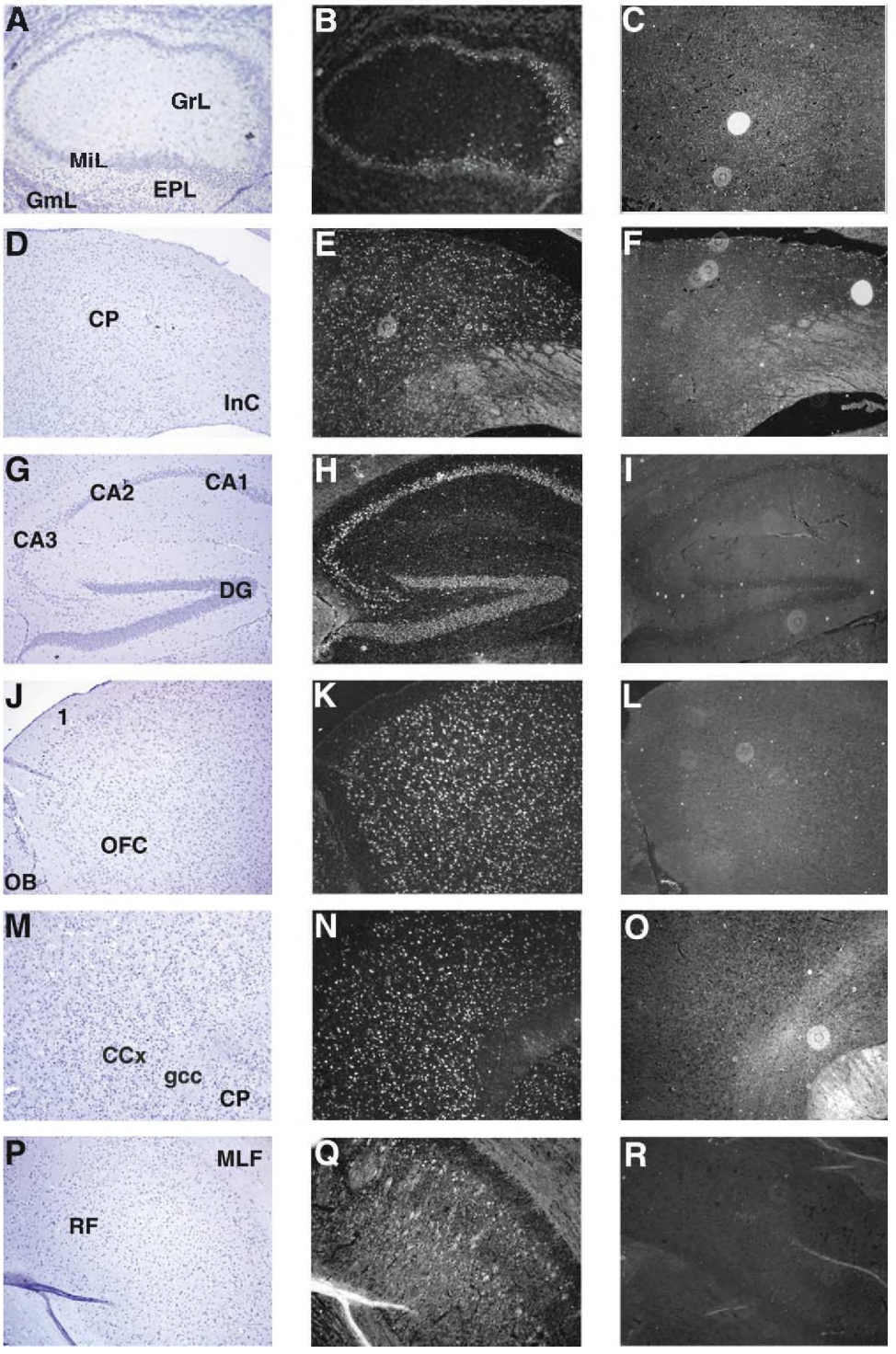

Figure 8. Expression Pattern of *Hoxb8* in the Adult CNS

In situ hybridization of the *Hoxb8* antisense riboprobe (left and middle columns) and of the control *Hoxb8* sense riboprobe (right column) to parasagittal sections of the brain from 8-month-old animals. In the left column are bright-field images demonstrating the hematoxylin counterstain; in the middle column are dark-field images of the same sections demonstrating the expression pattern of *Hoxb8* in each tissue. The right column contains dark-field images of sections adjacent to these shown in the other two columns. For all of the panels except (D)–(F), anterior is on the top of the image and ventral is on the left. For (D)–(F), anterior is on the right and ventral is on top of the images. (A–C) Olfactory bulb: GrL, granule cell layer; MiL, mitral cell layer; EPL, external plexiform cell layer; GmL, glomerular cell layer. (D–F) Caudate-putamen, CP; InC, internal capsule. (G–I) Hippocampus: DG, dentate gyrus. (J–L) Orbitofrontal cortex: OB, olfactory bulb; OFC, orbital frontal cortex; 1, cortex layer 1. (M–O) Anterior cingulate cortex, CCx; gcc, genu corpus collusum. (P–R) Brainstem: RF, reticular formation; MLF, medial longitudinal fisciculus.

mutants, as well as the adult CNS expression pattern of this gene, strengthen this argument. Videotape analysis has revealed that the excessive grooming observed in *Hoxb8* mutants is manifested in four ways, and in two distinct genetic backgrounds. First, all of the mutant animals display hair removal, and the more severely affected have self-inflicted open skin lesions. Significant amounts of hair loss and lesions were also reported in one-third of animals homozygous for the *lacZ* allele of *Hoxb8* (van den Akker et al., 1999). Second, the mutant animals were found to spend significantly more time grooming when compared to control littermates in both the home cage and in the induced grooming assay. Third, *Hoxb8* mutants were found to initiate grooming sequences more frequently than controls. Fourth, and most importantly, mutant animals excessively groomed their wild-type cagemates. The latter aspect of the phenotype suggests that peripheral nervous system deficits in the mutant mice are unlikely to be responsible for the excessive grooming behavior.

The cellular localization of *Hoxb8* within the adult CNS is consistent with studies linking grooming behaviors to specific regions of the brain (Aldridge et al., 1993; Berntson et al., 1988; Berridge, 1989a; Berridge and Fentress, 1987b; Berridge and Whishaw, 1992; Cannon, 1992; Cromwell and Berridge, 1996; McGrath et al., 1999; Robertson et al., 1999). In particular, decerebration studies have demonstrated that the brainstem is required for generation of the fixed-action patterns that characterize grooming behaviors (Berridge, 1989a). Animals that are decerebrated at the metencephalic level are capable of performing syntactic grooming chains. Furthermore, the neuronal circuitry that is responsible for generating grooming patterns does not appear to be confined to a single level within the brainstem; rather the neurons involved appear to be distributed throughout the entire structure. In addition, stimulation studies using electrodes implanted into the brainstem have demonstrated that comparable paleocerebellar circuits are involved in controlling behavioral responses such as grooming in opossums, rodents, and cats (Berntson et al., 1988). Interestingly, deafferentation of the trigeminal nerve has demonstrated that grooming behaviors are not dependent on tactile sensory feedback, implying that the self-mutilating behavior observed in *Hoxb8* mutants is not the result of altered sensory perception within the peripheral nervous system (Berridge and Fentress, 1987a).

Although the brainstem has been implicated in generation of the basic elements of grooming chains, numerous studies have demonstrated that the caudate-putamen region of the basal ganglia (commonly referred to as the neostriatum) is required for the implementation of the syntactic grooming chain. Both dopamine depletion, resulting from 6-hydroxydopamine-induced denervation of nigrostriatal dopamine projections, and loss of striatal intrinsic neurons due to injections of neurotoxic kanaic acid, caused a disruption in the implementation of syntactic grooming chains (Berridge, 1989b; Berridge and Fentress, 1987b). Additionally, electrophysiological recordings using implanted electrodes have shown that individual neurons within the anterior dorsolateral regions of the caudate-putamen are activated during grooming movements (Aldridge et al., 1993). And finally, the use of quinolinic acid to introduce small bilateral lesions has demonstrated that disruption of a single site in the anterior dorsolateral striatum results in deficits in syntactic chain completion (Cromwell and Berridge, 1996). These findings have led to the hypothesis that the basal ganglia play a modulatory role during grooming behaviors. Specifically, the striatum is believed to implement grooming behaviors by modulating the activation of other competing circuits, such as sensorimotor guided systems. As such, the striatum is acting to mediate a phasic shift over control of movement from sensorimotor guided systems to central pattern generating circuitry. This implies that the striatum acts in a hierarchical fashion to control neural circuitry during grooming and other innate behaviors. This hypothesis is supported by findings in other species as well. For example, in canines, innate behaviors such as grooming have been found to originate via activation of basal ganglia and limbic neurocircuits (MacLean, 1985a, 1985b; Stein et al., 1992; Wise and Rapoport, 1989). Additionally, studies in squirrel monkeys have shown that the basal ganglia are a repository for species-specific motor patterns (MacLean, 1978). The association between function of the striatum and the development, maintenance, and selection of both motor and cognitive responses has been recognized in many different species.

The excessive grooming behavior associated with the loss of *Hoxb8* function in mice is of potential clinical interest because of its possible relation to the etiology of human trichotillomania. The mouse and human pathologies are remarkably similar. There is controversy as to whether trichotillomania should be classified as an obsessive-compulsive disorder (OCD) or as an impulse-control disorder. Based on the expression pattern of *Hoxb8* in the CNS and the behavior analysis of affected animals, our work would favor classification of this disease as an OC-spectrum disorder. Functional imaging analysis has led to the description of an OCD circuit involving the basal ganglia and components of the neocortex (Graybiel and Rauch, 2000). The basal ganglia are connected to the neocortex by parallel loops of cortico-basal ganglia connections. Different sets of cortico-basal ganglia loops are believed to be associated with specialized functions depending on the cortical areas involved in the circuit. The OCD circuit links the orbitofrontal and anterior cingulate cortex to multiple sites in the striatum and limbic system. Additionally, the anterior cingulate cortex is connected to the motor cortex allowing for selected output of action in response to perceived stimuli. These cortico-basal ganglia circuits are believed to form a neural system that is required for habit learning, routine performance of these habits, and the acquisition of stereotyped behaviors (Graybiel, 1997). Abnormal function of this circuitry has been linked to the abnormal repetitive behaviors exhibited by patients afflicted with OCD and OC-spectrum disorders (Rauch and Baxter, 1998; Saxena et al., 1998). We have demonstrated expression of *Hoxb8*, in the principle components of the OCD circuit, which include the orbitofrontal cortex, the anterior cingulate cortex, the striatum, and the limbic system, as well as in other regions of the CNS associated with rodent grooming behavior. Thus we suggest that trichotillomania may arise from a misregulation of an innate autogrooming behavior re-

sulting in excessive repetition of this behavior and its associated pathology.

In summary, we have demonstrated that mice homozygous for a loss-of-function allele of *Hoxb8* show excessive grooming behavior that leads to pathology, removal of their own body hair, and self-inflicted wounding in the groomed areas. It will be of great interest to determine whether subsets of human patients with trichotillomania have defects in the *Hoxb8* gene or in paralogous family members, *Hoxc8* and *Hoxd8*. Furthermore, these *Hoxb8* mutant mice may provide an important animal model for pharmacological analysis of OCD-like phenotypes. Grooming is an ancient behavior common to vertebrates and invertebrates. It is interesting, and perhaps not fortuitous, that a member of an ancient set of genes, the *Hox* complex, is used to regulate this ancient behavior.

Experimental Procedures

Disruption of the *Hoxb8* Locus

An 11.2 kb DNA fragment that contained the *Hoxb8* gene was isolated from a genomic λDNA library prepared from a mouse 129Sv ES cell line and used to construct the *Hoxb8* targeting vector. Two different mutations were introduced into the *Hoxb8* locus. First, a unique BamH1 site in the first exon was converted to a ClaI site via restriction enzyme cleavage, followed by a fill-in and ligation resulting in a 4 bp insertion that produces a premature translation stop codon in the *Hoxb8* open reading frame. Second, a floxed *pMC-1neo*^{r} cassette was inserted into the second exon of *Hoxb8* at an XmnI site within the homeodomain. A total of 8.2 kb of *Hoxb8* genomic sequence surrounded the two mutations, and was inserted between the *TK1* and *TK2* genes to generate the *Hoxb8* targeting vector. This vector was linearized and electroporated into R1 ES cells. Cells that had undergone homologous recombination at the *Hoxb8* locus were enriched using positive-negative selection in medium containing G418 and FIAU (Mansour et al., 1988). Two of these ES cell lines were used to generate the chimeras that transmitted the *Hoxb8* mutations to their progeny.

Genotype Analysis

Pups and newborns were genotyped by PCR analysis of tail DNA. PCR primers were derived from within the *Hoxb8* homeobox (5′ primer, *Hoxb8*), sequences at the 3′ end of the *neo*^{r} gene (3′ primer, *neo*^{r}), and sequences near the 3′ end of the *Hoxb8* gene (3′ primer, *Hoxb8*). The sequence of each of the primers is as follows: 5′*Hoxb8*-5′CGAGGCCGCCAGACCTACAGT3′; 3′*Hoxb8*-5′CATTTACTGCTG GGAAACTTGTCT3′; 3′*neo*^{r}-5′GCCTGCTTGCCGAATATCATGG3′.

Skeletal Analysis and Whole-Mount In Situ Hybridization

Newborn and adult animals were collected and sacrificed via CO_2 asphyxiation. Skin was removed from the carcasses, and skeleton preparations were made as described (Mansour et al., 1993).

In situ antisense riboprobe hybridization of E9.5–E12.5 embryos was performed as described (Manley and Capecchi, 1995). The concentration of digoxigenin-UTP-labeled RNA was 0.4 mg/ml. The templates for *Hoxb9*, *Hoxb8*, and *Hoxb6* have been described previously (Chen and Capecchi, 1997; Rancourt et al., 1995).

Histological Analysis

The specimens were embedded in paraffin and 10 μm sections in the transverse orientation were mounted on slides. The sections were then stained with hematoxylin and eosin.

For adult skin, animals were sacrificed with CO_2 and shaved to remove the hair. Pieces of both ventral and lateral skin from the cervical, thoracic, and abdominal regions were removed using 3 mm skin biopsy punches. The biopsy was then flattened on a sterile paper towel and fixed for 4–6 hr in 10% formalin. The samples were embedded in paraffin, cross-sectioned at 10 μm, and stained with either hematoxylin and eosin, or giemsa.

Behavioral Analyses

Animals were housed in clear cages on a standard 12 hr light/dark cycle. Seven pairs of sex-matched littermates, one wild-type and one homozygous mutant in each pair, each individual in its own home cage, were placed in a locked room and videotaped (four male pairs, three female pairs) using a JVC camcorder and VCR for a single 24 hr period. Videotapes were changed every 8 hr.

The same 12 hr of videotape, distributed as three 4 hr blocks spread evenly throughout the 24 hr period, were examined for each animal (10 AM–2 PM; 6 PM–10 PM; 2 AM–6 AM). The amount of time each animal spent eating, grooming, and sleeping during a given analysis period was recorded and the total amount of time spent on each activity determined. During analysis of the videotapes, an individual grooming bout was recorded only if the bout contained all of the elements of a grooming sequence, lasted at least 30 s, and did not contain a pause of greater than 15 s.

During the induced grooming assay, sib pairs of wild-type and mutant mice were each placed in individual cages that did not contain bedding, food, or water. Following a 10 min acclimation period, the animals were lightly misted with water, and videotaped for a period of 20 min. This assay was repeated once each day on five consecutive days.

Detection of *Hoxb8* Transcripts

For the RT-PCR assay, animals were sacrificed by CO_2 asphyxiation, and the brain and cervical spinal cord rapidly dissected. Further dissection separated the cervical spinal cord, medulla, and pons from the rest of the adult brain. Following dissection, each tissue was placed in an Eppendorf tube containing tissue resuspension buffer (Qiagen RNeasy Kit) and broken up using a sterile disposable pestle. The samples were further disrupted using a QIA Shredder and total RNA samples were subsequently isolated using the Qiagen RNeasy Mini Kit.

cDNA synthesis and amplification of *Hoxb8* transcripts were performed using the PCR Access Kit (Promega). One hundred nanograms of total RNA was used for each reaction, and the sequence of the primers used to amplify either *Hoxb8* or the actin control were as follows: 5′RT*b8*-5′TCCAGCACCCTTCGCAAATCC3′; 3′RT*b8*-5′GTGCCCGCTCCAGCTTCTCTT-3′; 5′Actin-5′GTAACAATGCCAT GTTCAAT3′; 3′Actin-5′CTCCATCGTGGGCCGCTCTAG.

For determination of the cellular localization of *Hoxb8* in the adult brain, animals were asphyxiated by CO_2 and fixed via cardiac perfusion with cold 4% paraformaldehyde (PFA). Following perfusion, the brain and spinal cord were dissected and postfixed for at least 6 hr in 4% PFA. Samples were then transferred to a 1× PBS solution containing 5% sucrose for cryopreservation. The samples were cryopreserved for several days at 4°C during which the sucrose concentration was increased stepwise to 30%. The tissue was frozen in OCT, sectioned at 10 μm, and mounted onto SuperfrostPlus slides (VWR).

For detection of *Hoxb8* transcripts in sections of adult brains, the slides were warmed to room temperature and rehydrated by two washes in a calcium- and magnesium-free (CMF) 1× PBS solution, followed by treatment with proteinaseK (1 μg/ml in CMF-PBS) for 10 min at room temperature. The slides were then rinsed three times with CMF-PBS and refixed in 4% PFA for 20 min on ice. Next, the slides were washed with CMF-PBS, deacetylated in 0.25% acetic anhydride/0.1 M triethanolamine,10 min with stirring, and washed with 0.2× SSC, 10 min, again stirring. The slides were dehydrated in an ethanol (EtOH) series and allowed to air dry for 30 min. Hybridization buffer (50% formamide/2× SSC/10% Dextran sulfate/0.01% herring sperm DNA/0.02% SDS) was spread across the sections and subsequently prehybridized for 2–3 hr at 50°C. Following prehybridization, a digoxigenin-UTP-labeled *Hoxb8* riboprobe was diluted in hybridization buffer (0.5 μg/ml) and placed on the sections(Chen and Capecchi, 1997). To increase the specificity of the *Hoxb8* riboprobe, the following modifications were made: the restriction enzyme site at the 5′ end of the clone was changed from Sac1 to Not1 to generate a 5′ overhang following linearization, and the ratio of UTP:dig-UTP in the probe-generating transcription reaction was reversed to compensate for the low U content of the probe. Alternating sections were exposed to antisense or sense (control) riboprobes. The slides were heated to 85°C for 10 min, and hybridized overnight

at 55°C in a humid chamber. The next day, the slides were washed with a solution containing 4× SSC and 10 mM DTT for 1 hr at RT; 50% formamide with 2× SSC and 10 mM DTT for 30 min at 50°C; and 500 mM NaCl and 10 mM Tris-HCl (pH 7.4) with 1 mM EDTA (NTE) for 15 min at 37°C. Unbound RNA was removed with 10 μg/ml RNase A (Sigma) in NTE (30 min, 37°C), and the slides were washed with NTE, 2× for 15 min at 37°C; 2× SSC for 15 min at RT; and 0.1× SSC for 15 min at RT. Rinse in 100 mM Tris-HCl (pH 7.5)/150 mM NaCl (TS), and block with 5% normal sheep serum/0.03% Triton X-100 in TS for 30 min at RT. The secondary antibody (Gold-conjugated α-dig) was diluted 1:400 in 10% sheep serum/0.3%Triton in TS, placed on the sections, and incubated overnight at 4°C. The next morning wash with 100 mM Tris-HCl (pH 7.4)/150 mM NaCl/0.1% fish gelatin, three times for 5 min, postfix in 2% gluteraldehyde for 2 min, rinse with dH_20, five times for 30 s, and then ddH20, three times for 3 min, followed by incubation with the Silver Enhancing Kit (Ted Pella) for 20 min. Stop the reaction with 2.5% Na-thiosulfate, and rinse thoroughly in running water. Counterstain with hematoxylin, dehydrate using an EtOH series, coverslip, and examine by both bright- and dark-field microscopy.

Acknowledgments

We thank all members of the Capecchi laboratory's tissue culture support group and animal care facility for their expertise. Assistance from L. Oswald and D. Lim for manuscript preparation, R. Beglarian for behavioral analysis, K.M. Murphy for ISH on CNS sections, and B. Lauer and G. Jones for digital video production is appreciated. J.M.G. was supported by the Dee Fellowship and a NIH Genetics Training Grant.

Received October 9, 2001; revised November 26, 2001.

References

Aldridge, J.W., Berridge, K.C., Herman, M., and Zimmer, L. (1993). Neuronal coding of serial order: Syntax of grooming in the neostriatum. Psychol. Sci. *4*, 391–395.

Araki, K., Araki, M., Miyazaki, J., and Vassalli, P. (1995). Site-specific recombination of a transgene in fertilized eggs by transient expression of Cre recombinase. Proc. Natl. Acad. Sci. USA *92*, 160–164.

Berntson, G.G., Jang, J.F., and Ronca, A.E. (1988). Brainstem systems and grooming behaviors. Ann. NY Acad. Sci. *525*, 350–362.

Berridge, K.C. (1989a). Progressive degradation of serial grooming chains by descending decerebration. Behav. Brain Res. *33*, 241–253.

Berridge, K.C. (1989b). Substantia nigra 6-OHDA lesions mimic striatopallidal disruption of syntactic grooming chains: a neural systems analysis of sequence control. Psychobiol. *17*, 377–385.

Berridge, K.C., and Fentress, J.C. (1987a). Deafferentation does not disrupt natural rules of action syntax. Behav. Brain Res. *23*, 69–76.

Berridge, K.C., and Fentress, J.C. (1987b). Disruption of natural grooming chains after striatopallidal lesions. Psychobiol. *15*, 336–342.

Berridge, K.C., Fentress, J.C., and Parr, H. (1987). Natural syntax rules control action sequence of rats. Behav. Brain Res. *23*, 59–68.

Berridge, K.C., and Whishaw, I.Q. (1992). Cortex, striatum and cerebellum: control of serial order in a grooming sequence. Exp. Brain Res. *90*, 275–290.

Cannon, R.L., Paul, D.J., Baisden, R.H., and Woodruff, M.L. (1992). Alterations in self-grooming sequences in the rat as a consequence of hippocampal damage. Psychobiol. *20*, 205–218.

Capecchi, M.R. (1997). Hox genes and mammalian development. Cold Spring Harb. Symp. Quant. Biol. *62*, 273–281.

Chen, F., and Capecchi, M.R. (1997). Targeted mutations in hoxa-9 and hoxb-9 reveal synergistic interactions. Dev. Biol. *181*, 186–196.

Chen, F., and Capecchi, M.R. (1999). The paralogous mouse *Hox* genes, *Hoxa9*, *Hoxb9* and *Hoxd9*, function together to control development of the mammary gland in response to pregnancy. Proc. Natl. Acad. Sci. USA *96*, 541–546.

Cohen-Tannoudji, M., Vandormael-Pournin, S., Drezen, J., Mercier, P., Babinet, C., and Morello, D. (2000). lacZ sequences prevent regulated expression of housekeeping genes. Mech. Dev. *90*, 29–39.

Cromwell, H.C., and Berridge, K.C. (1996). Implementation of action sequences by a neostriatal site: a lesion mapping study of grooming syntax. J. Neurosci. *16*, 3444–3458.

Deschamps, J., and Wijgerde, M. (1993). Two phases in the establishment of HOX expression domains. Dev. Biol. *156*, 473–480.

Fentress, J.C. (1988). Expressive contexts, fine structure, and central mediation of rodent grooming. Ann. NY Acad. Sci. *525*, 18–26.

Godwin, A.R., and Capecchi, M.R. (1998). Hoxc13 mutant mice lack external hair. Genes Dev. *12*, 11–20.

Graybiel, A.M. (1997). The basal ganglia and cognitive pattern generators. Schizophr. Bull. *23*, 459–469.

Graybiel, A.M., and Rauch, S.L. (2000). Toward a neurobiology of obsessive-compulsive disorder. Neuron *28*, 343–347.

Guy, L.G., Kothary, R., and Wall, L. (1997). Position effects in mice carrying a lacZ transgene in cis with the beta-globin LCR can be explained by a graded model. Nucleic Acids Res. *25*, 4400–4407.

Horwath, E., and Weissman, M.M. (2000). The epidemiology and cross-national presentation of obsessive- compulsive disorder. Psychiatr. Clin. North Am. *23*, 493–507.

Le Mouellic, H., Lallemand, Y., and Brulet, P. (1992). Homeosis in the mouse induced by a null mutation in the Hox-3.1 gene. Cell *69*, 251–264.

MacLean, P.D. (1978). Effects of lesions of globus pallidus on species-typical display behavior of squirrel monkeys. Brain Res. *149*, 175–196.

MacLean, P.D. (1985a). Brain evolution relating to family, play, and the separation call. Arch. Gen. Psychiatry *42*, 405–417.

MacLean, P.D. (1985b). Evolutionary psychiatry and the triune brain. Psychol. Med. *15*, 219–221.

Manley, N.R., and Capecchi, M.R. (1995). The role of *hoxa-3* in mouse thymus and thyroid development. Development *121*, 1989–2003.

Mansour, S.L., Goddard, J.M., and Capecchi, M.R. (1993). Mice homozygous for a targeted disruption of the proto-oncogene *int-2* have developmental defects in the tail and inner ear. Development *117*, 13–28.

Mansour, S.L., Thomas, K.R., and Capecchi, M.R. (1988). Disruption of the proto-oncogene int-2 in mouse embryo-derived stem cells: a general strategy for targeting mutations to non-selectable genes. Nature *336*, 348–352.

McGrath, M.J., Campbell, K.M., and Burton, F.H. (1999). The role of cognitive and affective processing in a transgenic mouse model of cortical-limbic neuropotentiated compulsive behavior. Behav. Neurosci. *113*, 1249–1256.

Odenwald, W.F., Taylor, C.F., Palmer-Hill, F.J., Friedrich, V., Jr., Tani, M., and Lazzarini, R.A. (1987). Expression of a homeo domain protein in noncontact-inhibited cultured cells and postmitotic neurons. Genes Dev. *1*, 482–496.

Rancourt, D.E., Tsuzuki, T., and Capecchi, M.R. (1995). Genetic interaction between *hoxb-5* and *hoxb-6* is revealed by nonallelic noncomplementation. Genes Dev. *9*, 108–122.

Rauch, S., and Baxter, L. (1998). Neuroimaging of OCD and related disorders. In Obsessive-Compulsive Disorders: Practical Management, M. Jenike, L. Baer, and W. Minichiello, eds. (Boston: Mosby), pp. 289–317.

Richmond, G., and Sachs, B.D. (1980). Grooming in Norway rats: the development and adult expression of a complex motor pattern. Behaviour *75*, 82–96.

Robertson, B.J., Boon, F., Cain, D.P., and Vanderwolf, C.H. (1999). Behavioral effects of anti-muscarinic, anti-serotonergic, and anti-NMDA treatments: hippocampal and neocortical slow wave electrophysiology predict the effects on grooming in the rat. Brain Res. *838*, 234–240.

Sachs, B.D. (1988). The development of grooming and its expression in adult animals. Ann. NY Acad. Sci. *525*, 1–17.

Sarna, J.R., Dyck, R.H., and Whishaw, I.Q. (2000). The Dalila effect:

C57BL6 mice barber whiskers by plucking. Behav. Brain Res. *108*, 39–45.

Saxena, S., Brody, A.L., Schwartz, J.M., and Baxter, L.R. (1998). Neuroimaging and frontal-subcortical circuitry in obsessive-compulsive disorder. Br. J. Psychiatry Suppl. *35*, 26–37.

Stein, D.J., Shoulberg, N., Helton, K., and Hollander, E. (1992). The neuroethological approach to obsessive-compulsive disorder. Compr. Psychiatry *33*, 274–281.

Strozik, E., and Festing, M.F. (1981). Whisker trimming in mice. Lab. Anim. *15*, 309–312.

Thomas, K.R., and Capecchi, M.R. (1987). Site-directed mutagenesis by gene targeting in mouse embryo-derived stem cells. Cell *51*, 503–512.

Thorey, I.S., Meneses, J.J., Neznanov, N., Kulesh, D.A., Pedersen, R.A., and Oshima, R.G. (1993). Embryonic expression of human keratin 18 and K18-beta-galactosidase fusion genes in transgenic mice. Dev. Biol. *160*, 519–534.

van den Akker, E., Reijnen, M., Korving, J., Brouwer, A., Meijlink, F., and Deschamps, J. (1999). Targeted inactivation of Hoxb8 affects survival of a spinal ganglion and causes aberrant limb reflexes. Mech. Dev. *89*, 103–114.

Wise, S., and Rapoport, J. (1989). Obsessive-compulsive disorder: is it basal ganglia dysfunction? In Obsessive-Compulsive Disorders in Children and Adolescents, J. Rapoport, ed. (Washington, DC: American Psychiatric Press), pp. 327–344.